DOI: 10.17344/acsi.2019.5093 *Acta Chim. Slov.* **2019,** *66,* 888–898

Scientific paper

Sulfate Ion Removal from Water Using Activated Carbon Powder Prepared by *Ziziphus Spina-Christi* Lotus Leaf

Morteza Rahmati,[1] Golan Yeganeh[2] and Hossein Esmaeili[3,*]

[1] *Department of Chemical Engineering, Datshtestan Branch, Islamic Azad University, Dashtestan, Iran*

[2] *Young Researchers and Elite Club, Bushehr Branch, Islamic Azad University, Bushehr, Iran*

[3] *Department of Chemical Engineering, Bushehr Branch, Islamic Azad University, Bushehr, Iran*

* *Corresponding author: E-mail: esmaeili.hossein@gmail.com & esmaeili.hossein@iaubushehr.ac.ir*

Received: 02-28-2019

Abstract

In this paper, the adsorption potential of activated carbon prepared by *Ziziphus spina-christi* lotus leaf for the removal of sulfate from aqueous solution was investigated. To this end, the effect of different parameters such as pH, contact time, temperature, adsorbent concentration, and initial sulfate ion concentration was investigated. The results indicated that the highest adsorption efficiency (84.5%) was obtained at pH 6, adsorbent concentration of 5 g/L, sulfate ion concentration of 20 ppm, 65 min and temperature of 45 °C. Also, the adsorption equilibrium study showed that the adsorption process follows the Langmuir isotherm model with the maximum adsorption capacity of 9.3 mg/g. In addition, the thermodynamic study showed that the adsorption process on the activated carbon surface was spontaneous. Moreover, the adsorption process was exothermic accompanied by a decrease in irregularity. Furthermore, the adsorption kinetic study indicated that the adsorption process follows the pseudo-second-order kinetic model.

Keywords: Adsorption; lotus leaf; sulfate ion; water purification

1. Introduction

Industrial and urban effluents are one of the main pollutants which can cause environmental pollution.[1] Among the pollutants, sulfate is one of the significant inorganic pollutants found in urban effluents and with different amounts in industrial wastewaters; its concentration in lakes and seas is increasing quickly due to the urban and industrial effluents drainage.[2]

When too much sulfate gets into the human stomach, it endangers health. Sulfate along other minerals cause pipe corrosion. Also, it may cause undesirable taste in water, diarrhea in human and young livestock. The taste threshold varies between 250 mg/L sodium sulfate and 1000 mg/L calcium sulfate. The undesirable taste of water usually gets reduced at values below 250 mg/L. Also, the maximum desirable amount of sulfate in drinking water is 250 mg/L and its maximum permitted is 400 mg/L.[3]

Several methods such as distillation, reverse osmosis, ion exchange, and adsorption are available for sulfate removal from water.[4] Physicochemical treatment systems such as ion exchange, reverse osmosis and electrodialysis are costly and produce sludge, which is difficult to dispose.[5] Adsorbents are widely used among many technologies for the removal of anions from water. Also, the adsorption method is economically feasible, frequent, diverse, effective, simple and eco-friendly.[6–9] In recent years, many researchers have been attracted to cheap adsorbents.[8–15] The use of activated carbon has been introduced as a widely used method for sulfate removal due to its efficiency and easy usage.[6]

Any carbon material can be used to produce activated carbon. Up to now, several studies have been conducted using activated carbon derived from agricultural wastes such as peanut crust, nuts shell, tamarind shell, peanut shell,[16] rice bran, rice hulls, banana peel, orange peel, apple peel, hazelnut, walnut shell, tree's leaf and bark, oak essence, cane bagasse, corn, wheat bran, sawdust, sunflower stem, grape stem, modified algae, alfalfa and mustard[13–15,17–27] for the removal of pollutants from wastewater.

In this work, the activated carbon powder obtained from lotus leaf was used to remove sulfate ion from aqueous solution and the effect of different parameters such as temperature, contact time, pH, adsorbent concentration

and sulfate ion concentration in aqueous solution were investigated and also, the optimum operational conditions for getting maximum adsorption was obtained. Lotus or Cedar is a plant from jujube family which grows wildly in Saudi Arabia, North Africa and Southern Iran which is used in this work.[28] Therefore, this plant is economically preferred a lot. Also, the adsorbent surface properties were studied via different analyses such as SEM, EDAX, FTIR, BET, and XRD. Eventually, the kinetic, equilibrium and thermodynamic studies of adsorption process were carried out and the adsorption process characteristics were investigated.

2. Materials and Method

2. 1. Chemical

In this work, sodium sulfate decahydrate with a purity of 99% was purchased from Merck Co., Germany. The HCl and NaOH made by Merck Co. (Germany) were also used to adjust the pH of the samples.

2. 2. Stock Solution

In order to prepare a stock solution containing sulfate ion, a certain amount of sodium sulfate decahydrate was poured into a 250 ml Erlenmeyer and double-distilled water was added to it to reach a volume of 100 ml. Standard solutions with low sulfate concentrations were prepared through diluting a certain volume of this stock solution using double-distilled water.

2. 3. Preparation of Lotus Leaf Powder

In order to prepare activated carbon adsorbent from lotus leaf, first, the leaves were washed with a lot of distilled water to remove dust. Then, they were placed in an oven at 100 °C for 60 minutes to completely dry. The dried leaves were placed in a furnace under 700 °C for 2 hours until they turned to charcoal. After carbonization, the leaves turned to powder by milling and graded through sieve No.25 then stored inside anti-moisture plastic bottles.

2. 4. Adsorbent Analysis

BET, SEM, FT-IR, EDAX, and XRD analyses were used to determine structural and morphological properties of activated carbon produced from Lotus leaves. In order to determine the functional groups in the adsorbent, the FT-IR Perkin device was used; surface structure and adsorption morphology was determined by SEM (Philips-x130), the XRD device made by GNR Npd3000 company was used to determine the adsorbent crystalline phases, the EDAX device (Philips-x130) was used to determine the adsorbent elements and the adsorbent specific surface area was determined through BET device (Philips model, USA).

2. 5. Adsorption Experiments

Adsorption experiments were conducted in a batch manner. To do this, the effect of sulfate ion concentration (20, 40, 60, 80, 100 and 120 mg/L), contact time (5 to 80 minutes), adsorbent dose (1–10 g/L), pH (4 to 10) and temperature (25, 35, 45, 55, 65 and 75 °C) on the sulfate ion adsorption from aqueous solution was investigated. In all experiments, the mixing speed was considered 200 rpm. The residual sulfate ion in the solution was obtained by spectrophotometer (DR 5000 Hach, USA). To this end, 10 mL sample volume containing sulfate ion was added to the device to measure the remaining sulfate at a wavelength of 450 nm.

First, in order to get the optimum pH, 7 samples of 100 ml aqueous solution containing 100 ppm sulfate ion were prepared. Then, the pH of the solutions was adjusted by NaOH (I M) and HCl (1 M) at the pH values from 4 to 10. After that, 5 g/L of activated carbon adsorbent was added to each sample containing sulfate ions and stirred by a magnetic stirrer with a mixing rate of 200 rpm at room temperature for 60 min. Then, the solution was filtered by Whatman filter paper, the adsorbent was removed and the amount of residual sulfate ion was obtained within the solution. The sulfate adsorption percentage by the adsorbent (%A) is calculated for each sample using equation (1), so the best pH value for maximum removal efficiency was achieved.

$$\%A = = \left(\frac{Ci-Co}{Ci}\right) \times 100 \quad (1)$$

where C_i and C_o (mg/L) are the initial concentration and the equilibrium concentration of the metal ion.

In order to investigate the adsorbent concentration effect in aqueous solutions, the effect of different concentrations of 1 to 10 g/L were considered. After that, 5 g/L of adsorbent was added to each aqueous solution with different concentrations at optimum pH; the solutions were stirred by magnetic stirrer with a mixing rate of 200 rpm at 25 °C for 60 min. After a specific time, the process was stopped and the solution was filtered by Whatman filter paper (No. 42) and the adsorbent was separated from the solution. Then, the residual sulfate ion in the solution was obtained and the best adsorbent concentration that is most adsorbed was determined. In order to determine the effect of other parameters, the same actions were performed. At each stage, in order to examine each parameter, other parameters considered as constant and the optimum values in the previous stage were used.

3. Results and Discussion

3. 1. Characteristics of the Adsorbent

BET analysis determines the specific surface area of the adsorbent (cavities identification and surface roughness). Working with this device is based on measuring the amount of neutral gas adsorption, such as nitrogen, at a

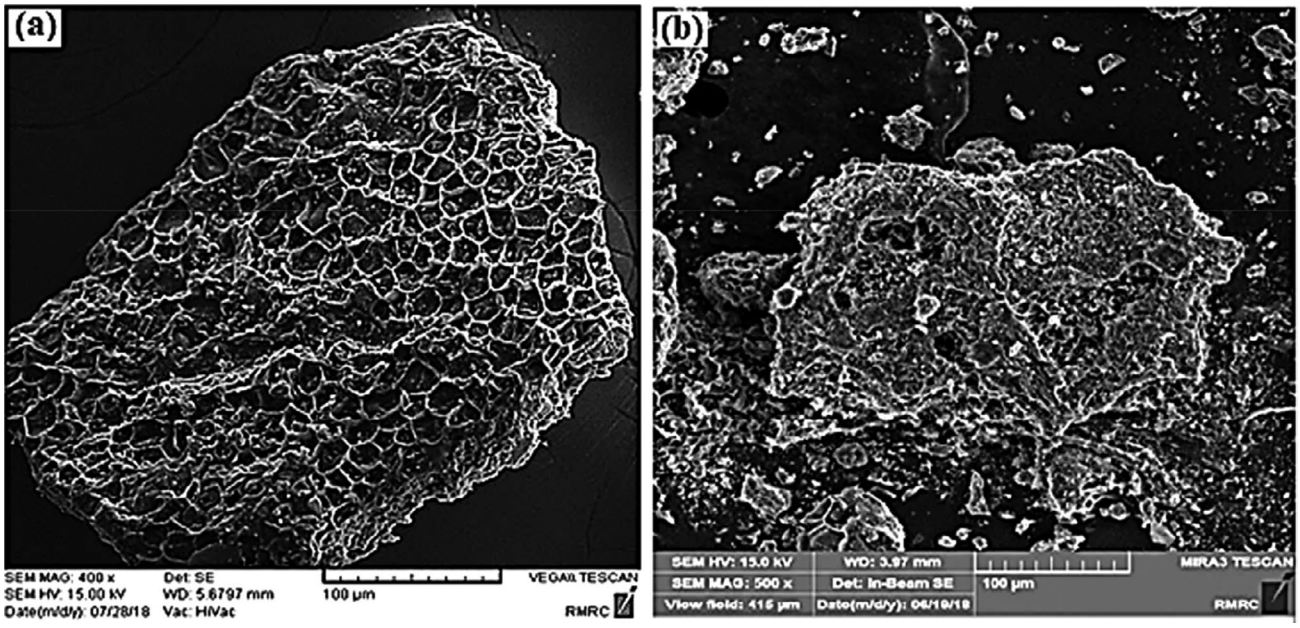

Figure 1. SEM analysis of adsorbent before (a) and after adsorption (b)

constant temperature on the adsorbent surface. The results showed that the adsorbent surface area of the lotus leaf is 51.024 m^2/g. Also, the average pore diameter (ADP) and the total pore volume (TPV) of Lotus leaf adsorbent are obtained 196.573 A and 0286800 cm^3/g.

SEM device was used to identify the adsorbent structure and morphology before and after the sulfate ion adsorption process. SEM images of the Lotus leaf adsorbent before and after adsorption are shown in Fig.1. As known, there are many roughness and cavities on the adsorbent surface which leads to adsorbent surface area increase representing different sites for sulfate ion adsorption. These cavities are coated after sulfate ion adsorption process which is clearly shown in the figure.

Fig. 2 shows the XRD pattern of the lotus leaf adsorbent. The spectra in 2 29 and 40° are related to Calcium Carbonate and the spectra in 2θ 28 and 34° are related to Potassium Chloride. According to Debye-Scherrer equation, the average diameters of Lotus leaf adsorbent crystals were determined 25.12 nm. Also, the spectra in 2θ 0.499 and 0.998 are related to empty cavities in the adsorbent.

Also, in the XRD analysis after adsorption, spectra in 2θ 29 and 40° are related to Calcium Carbonate and the spectra in 2θ 28 and 34° are related to Potassium Chloride. According to Debye-Scherrer equation, the average diameters of Lotus leaf adsorbent were determined 29.88 nm. Also, the spectra in 2θ 0.499 and 0.998 are related to empty cavities in the adsorbent sample. By comparing the graphs before and after adsorption, it can be seen that both graphs have very similar peaks which shows that the adsorbent structure has not changed much after adsorption.

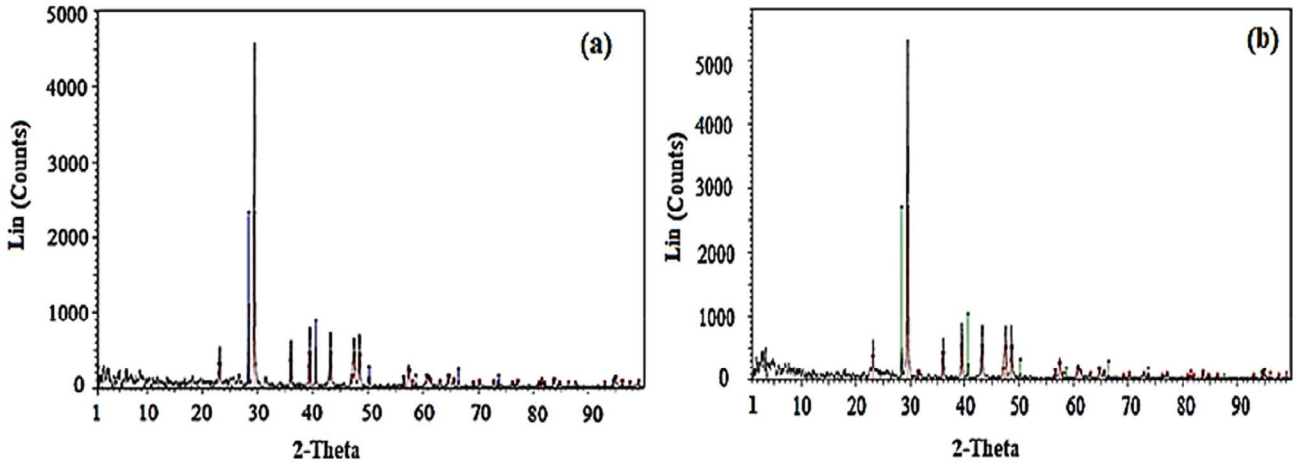

Figure 2. XRD analysis of activated carbon adsorbent before (a) and after adsorption (b)

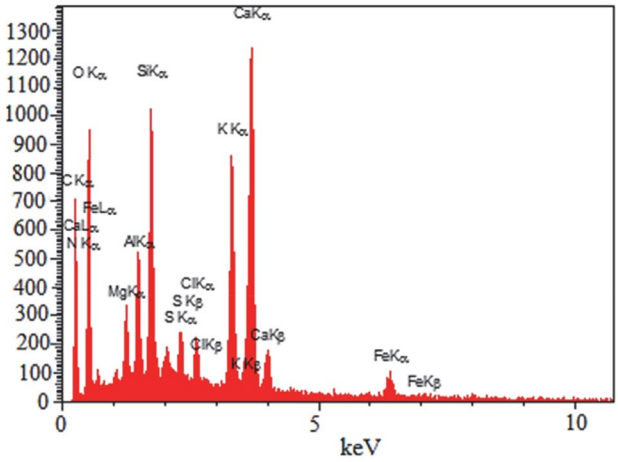

Figure 3. EDAX analysis of activated carbon adsorbent

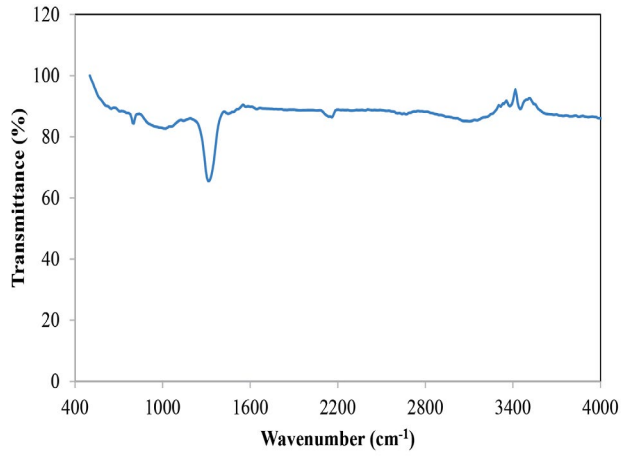

Figure 4. FT-IR analysis of activated carbon adsorbent

Also, the EDAX analysis on the Lotus leaves for the adsorbent elements determination is shown in Fig. 3 and Table 1. As is evident in the Fig, there are various elements such as Fe, Ca, K, Cl, S, Si, Al, Mg, O, C, N in the Lotus leaf sample which their weight percentage are 2.39, 11.96, 6.81, 1.15, 1.22%, 4.40, 2.11, 1.39, 38.89, 25.80 and 3.86%, respectively. So, the most important components in its structure were oxygen and carbon.

Table 1. Elemental analysis of the adsorbent by EDX apparatus

Elements	Weight (%)	Atomic (%)
C	25.80	37.47
N	3.86	4.81
O	38.89	42.40
Mg	1.39	1.00
Al	2.11	1.37
Si	4.40	2.73
S	1.22	0.66
Cl	1.15	0.57
K	6.81	3.04
Ca	11.96	5.20
Fe	2.39	0.75
Total	100.00	100.00

Also, the FTIR analysis results for functional groups determination in the 400–4000 cm^{-1} range are shown in Fig. 4. The results show that the spectrum of 798.795 $cm^{-1}$is related to the aromatic tensile bond of –C–H, 1016.45 cm^{-1} frequency shows the C–O group (carboxylic acid), 1315.19 cm^{-1} frequency shows the C-F functional group, 2158.81 cm^{-1} frequency shows the functional group of C ≡ C, 3101.21 cm^{-1} frequency shows the H–O (alcohol) functional group and the frequency of 3451.37 cm^{-1} shows the N–H functional group (amide).

3. 2. The pH Effect on Adsorption

The initial pH of the solution containing sulfate ions affects the changes in surface charge of the adsorbent and the adsorption mechanism of sulfate ions in the adsorption process.[29] Also, the initial pH of the solution is considered as one of the important parameters during the adsorption process.[30] Because the existing hydrogen ions (H^+) in the aqueous solution compete with other ions to sit on the adsorbent surface. Also, the initial pH of the solution affects the variations of adsorbent surface charge and ionization degree of the adsorbed material (sulfate) during the adsorption process. The pH effect on the SO_4^{2-} ion adsorption on the activated carbon surface derived from lotus leaf is shown in Fig. 5.

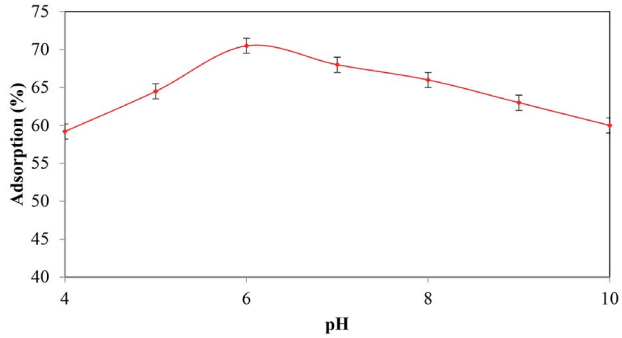

Figure 5. The pH effect on the SO_4^{2-} ion adsorption using the activated carbon derived from lotus leaf (Other conditions: T = 298 K, m = 0.5 g, Tc = 60 min, SO_4 = 100 mg/l)

As shown in the figure, the sulfate ion adsorption efficiency increases by raising pH from 4 to 6. Since the ambient is acidic at low pH, so, the Hydrogen ions concentration in the aqueous solution is high and since the hydrogen ion is placed on the adsorbent surface, the adsorbent load gets positive; therefore, the electrostatic force makes adsorption between the adsorbent positive load and Sulfate anion negative load. The maximum percentage of sulfate ion adsorption happens at pH = 6. Sulfate anion is better adsorbed at low pHs. After that, sulfate adsorption decreases. The maximum adsorption of sulfate ion

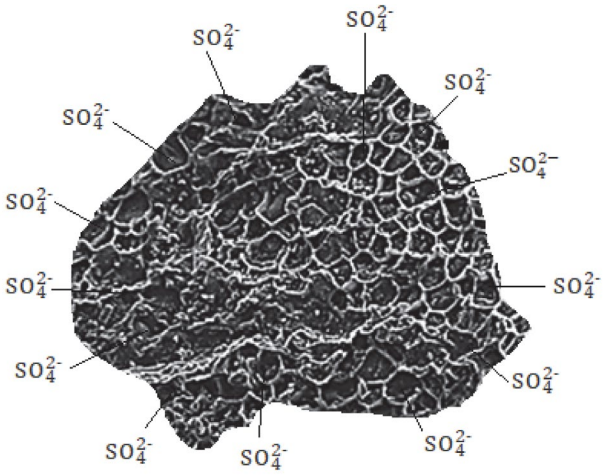

Figure 6. The adsorption mechanism of sulfate ions on the active sites of the activated carbon

through Lotus leaf was obtained 70.5%. The adsorption efficiency decreased after pH = 6 and by changing the pH from 6 to 10, sulfate ion adsorption percentage decreased from 70.5 to 60%. At this point, the hydroxide ion concentration increases inside the solution which leads to $SO_4(OH^-)$ hydrolysis, complex formation and sulfate ion sedimentation is as $SO_4(OH_2)$ Due to the sediment and complex formation, sulfate ions decreased in the aqueous solution, subsequently reduced the adsorption efficiency. Fig. 6 shows the adsorption mechanism of sulfate ions for sitting on the active sites of the adsorbent.

3. 3. The Effect of Adsorbent Dose

Adsorption dose is one of the important parameters on the adsorption process because it represents the maximum adsorption rate.[31] The effect of adsorption dose on the sulfate ion adsorption efficiency is shown in Fig. 7. According to the graph, increasing the adsorbent concentration from 1 to 5 g/L caused significant changes in adsorption. By increasing the adsorbent dose from 1 to 5 g/L, sulfate ion adsorption percentage increases from 45 to

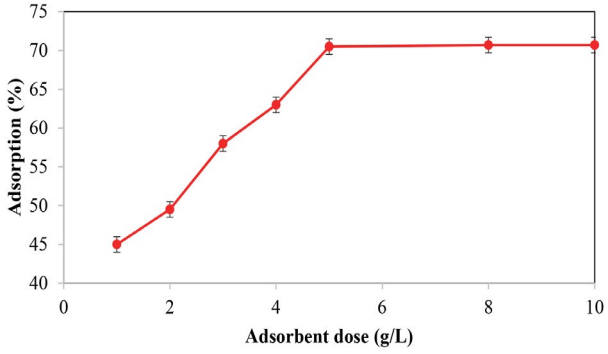

Figure 7. The effect of the adsorbent dose on the adsorption of sulfate ion (T = 298 K, pH = 6, Tc = 60 min, SO_4 = 100 mg/L)

70.5%. Also, at concentration more than 5 g/L, no change in adsorption was observed. The increase in slope at the beginning of the graph is mainly due to the increase of adsorbent surface area and a large number of active sites for sulfate ion adsorption.

3. 4. The Contact Time Effect on the Adsorption Amount

The effect of contact time on the adsorption of sulfate ion from aqueous media using activated carbon prepared by lotus leaf is shown in Fig. 8.

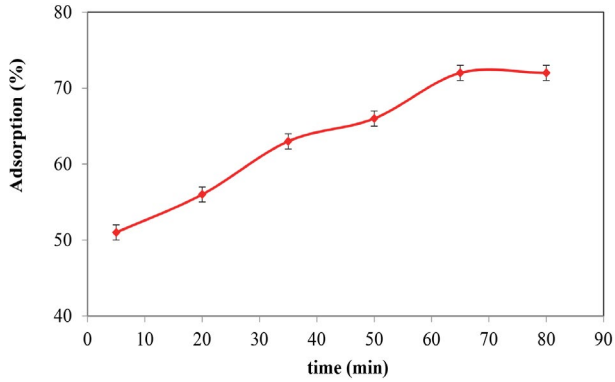

Figure 8. The effect of contact time on the adsorption of sulfate ion (T = 298 K, m = 0.5 g, pH = 6, sulfate ion concentration = 100 mg/L)

According to the figure, the optimum time for SO_4^{2-} ion adsorption on the active carbon surface is 65 minutes. For sulfate ion adsorption as shown in the graph, the graph's slope gets sharper by increasing the contact time, the slope steepness means that adsorption has occurred at high rate, because many active sites on the adsorbent surface are empty at the beginning of the sulfate ion adsorption process through Lotus leaf adsorbent and sulfate is placed on the sites. Therefore, the removal percentage has been increased by increasing the contact time; the graph's slope remained constant after 65 minutes and sulfate removal percentage got balanced. After 65 min, the sulfate removal efficiency remained constant due to the saturation of adsorbent active sites. Therefore, the contact time of 65 min was considered as the optimum time for sulfate ion adsorption.

3. 5. Temperature Effect

Another important parameter in the adsorption process is temperature. This parameter indicates that the adsorption process is exothermic or endothermic. The temperature effect on SO_4^{2-} ion adsorption on the active carbon surface is shown in Figure 9.

According to the figure, when temperature increases from 298 to 348 K, the sulfate removal percentage by the

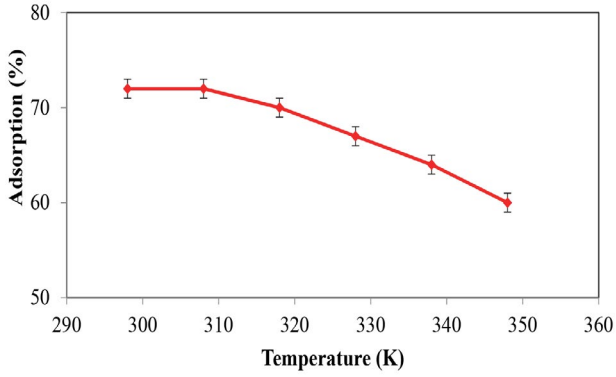

Figure 9. Temperature effect over SO_4^{2-} ion adsorption on the activated carbon derived from lotus leaf (Other terms: Tc = 65 min, m = 0.5 g, pH = 6, SO_4 = 100 mg/L)

adsorbent decreases. This percentage decrease is due to the molecular movement reduction. The adsorption reaction rate decreases by the molecular movement reduction. On the other hand, according to le Chatelier principle, adsorption level decreases when the temperature rises. This is somehow associated with irregularities reduction. The adsorption capacity reduction by temperature increase represents an exothermic reaction. Therefore, the optimum adsorption temperature for SO_4^{2-} ion is 298 K.

3. 6. The Initial Concentration of SO_4^{2-} Ion

In the adsorption process, the initial concentration of metal ions in aqueous solution plays an important role as the mass transfer force between the solution and solid phase (adsorbent). The sulfate ion concentration effect on the removal from aqueous solution is shown in Fig. 10. At initial concentrations, the ratio of active sites to the initial concentration of sulfate in aqueous solution raises, so, the

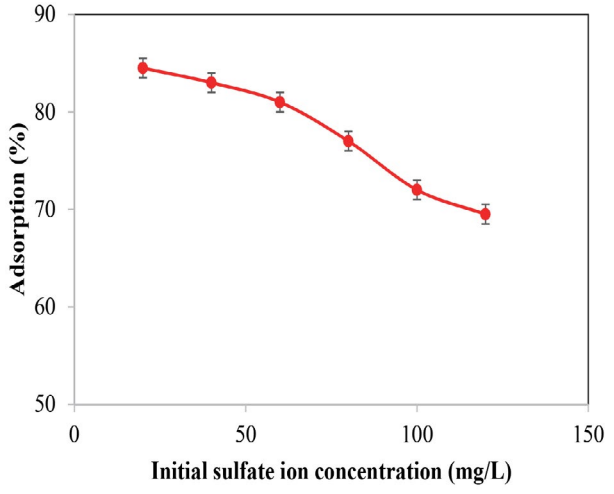

Figure 10. The investigation of SO_4^{2-} ion's initial concentration on the adsorption over the carbon surface derived from Lotus leaf (Other conditions: T = 298 K, m = 0.5 g, pH = 6, Tc = 65 min)

interaction between adsorbent and sulfate ion increases and anion gets removed from aqueous solution. The adsorption efficiency of sulfate ion decreased by increasing the initial sulfate ion concentration which is ascribed to the competition of sulfate ion to sit on active sites of the adsorbent. Also, the ions in the aqueous solution can be able to be interacted with prepared adsorbent and be removed from the aqueous solution.[17] Therefore, the initial ion concentration of 20 mg/L with an adsorption efficiency of 84.5 was considered as an optimum value.

3. 7. Adsorption Isotherm Study

The adsorption isotherm study presents information about the effective interaction between adsorbent and the absorbed. In order to evaluate the equilibrium adsorption, the Langmuir, Freundlich, Temkin and Dubinin-Radushkevich isotherm models were studied. The Langmuir adsorption isotherm is used for monolayer adsorption on surfaces with limited identical adsorption positions. The linear form of this model is described as follows:[29,32]

$$\frac{1}{q_e} = \frac{1}{K_L q_m}\left(\frac{1}{C_e}\right) + \frac{1}{q_m} \quad (2)$$

For determining the K_L and q_m, the slope and intercept of $1/q_e$ based on $1/C_e$ can be used. One of the based uses of Langmuir's constant is to determine the separation factor (R_L) according to Equation (3). If $R_L > 1$, $R_L = 0$ or $0 < R_L < 1$, the process will be undesirable, irreversible, linear and desirable, respectively.[33]

$$R_L = \frac{1}{1 + K_L C_i} \quad (3)$$

Also, the Freundlich isotherm describes the adsorption on inhomogeneous surfaces with uniform energy sites. The linear form of Freundlich isotherm follows from Equation 4.[33]

$$\log q_e = \log K_f + \frac{1}{n}\log C_e \quad (4)$$

In this equation, if 1/n is between zero and one, it shows that the adsorption process intensity is non-uniform at all levels. If 1/n is less than one, it shows that the adsorption process has been chemical and when 1/n value is more than 1, the adsorption process will be physical.

In these equations, q_e is the amount of adsorbed pollutant (mg/g) at the equilibrium time, q_m is the maximum adsorption capacity by adsorbent (mg/g), C_e is the equilibrium concentration of absorbed component (mg/L) and K_L is the equilibrium constant (L/mg) which depends on the degree of absorbed component tendency towards adsorbent; K_F and n are Freundlich isotherm constants which represent the capacity and intensity of adsorption, respectively.

In the Langmuir model, K_L and q_m are obtained from the slope and intercept of $1/q_e$ based on $1/C_e$. Also, in the

Freundlich model, K_F and n are calculated from the slope and intercept of log q_e versus log C_e.

Temkin model is another isothermal model. In this double-parameter model, it is assumed that the adsorption is monolayer and heterogeneous. The linear form of this model is as follows:

$$q_e = B_T LnA_T + B_T LnC_e \quad (5)$$

A_T is the Temkin constant based on (L mg^{-1}) and it is compatible with adsorbent-absorbed adhesion.

The B_T constant is defined as $B_T = \frac{RT}{K_T}$. K_T is the Temkin constant based on (J mol^{-1}) which is proportionate with adsorption heat. The A_T and B_T amounts are calculated from the slope and intercept of q_e based on ln C_e.

The Dubinin-Radushkevich (D-R) isotherm model which is a semi-experimental relation. It assumes that the adsorption process is monolayer, so, it can be both chemical and physical. This model assumes that the surface is uneven, it has a linear form as follows:

$$Lnq_e = Lnq_d - K_D\varepsilon^2 \quad (6)$$

Here, q_d is the D-R isotherm constant which is proportionate with saturation capacity expressed by mg g^{-1}. K_D is another constant based on (mol J^{-1})^2 expressed by $E = -0.7\ K_D^{-0.5}$. More negative free energy means the adsorption is more chemical. Finally, ε represents the Polanyi potential (J/mol) defined by the $\varepsilon = RTLn(1+\frac{1}{C_e})$ equation. This is calculated by drawing *Ln* q_e graph based on ε^2, and q_d and K_D are measured by its slope and intercept.[34]

The isothermal results are shown in Tables 2 and 3 and Figure 11. According to these results, the correlation coefficient (R^2) in Langmuir isotherm model is higher than other models and also closer to 1; showing that Langmuir isotherm model has more capability for describing the isothermal behavior of adsorption process which also indicates the monolayer adsorption nature of sulfate ion

Table 2. The results of various isotherms of SO_4^{2-} ion adsorption on the activated carbon surface derived from Lotus leaf (Other terms: T = 298 K, m = 0.5 g, pH = 6, Tc = 65min)

Isotherm	Parameter	value
Langmuir	q_m (mg/g)	9.3
	K_L (L/mg)	0.2
	R^2	0.9742
	n	0.61
Freundlich	$K_F(mg)^{1-n}$ L^n g^{-1}	2.0
	R^2	0.8719
	A_T (L mg^{-1})	1.1
Temkin	B_T	10.576
	R^2	0.6071
	q_d (mg/g)	15.6
D-R	$K_D \times 10^{-6}$ (mol/J)^2	6.0
	E (kJ/mol)	–903.7
	R^2	0.7801

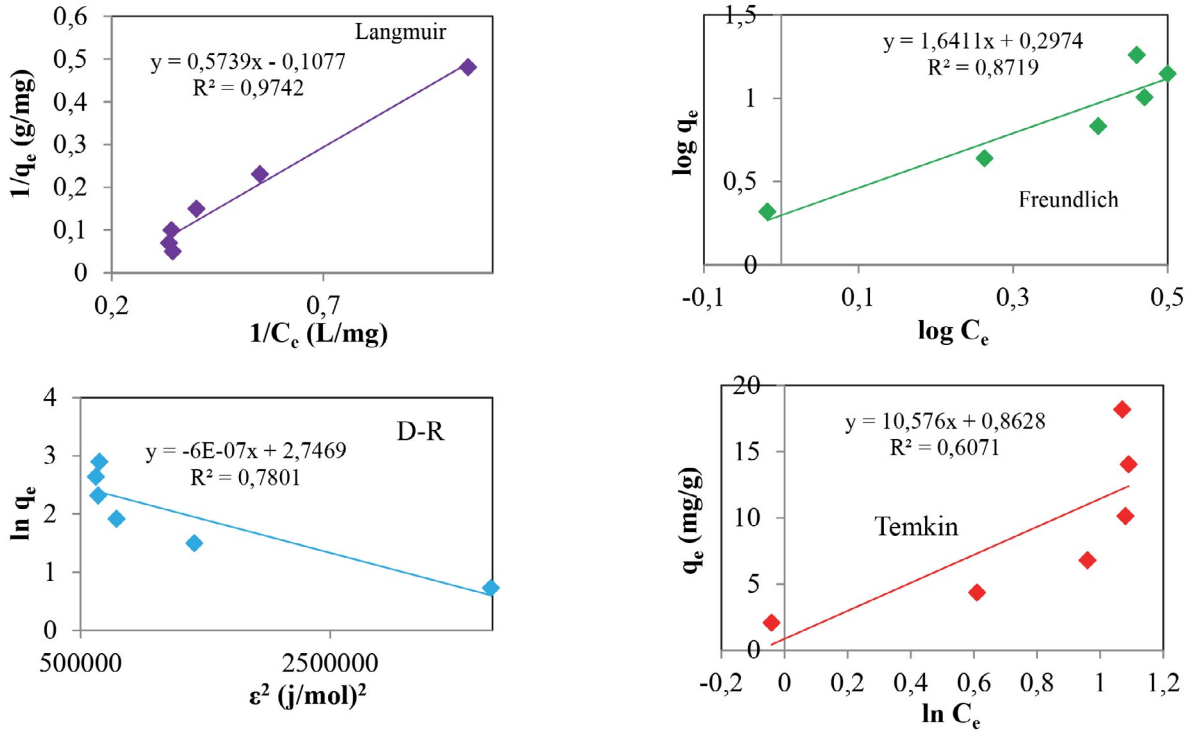

Figure 11. Adsorption isotherms of SO_4^{2-} ion on the activated carbon surface including Langmuir, Freundlich, Temkin, and Dubinin-Radushkevich isotherms

Table 3. The amount of adsorption separation factor of various SO_4^{2-} ion concentrations on the activated carbon surface derived from Lotus leaf, regarding the R_L

Initial ion concentration (mg/L)	20	40	60	80	100	120
R_L	0.71	0.6	0.5	0.4	0.33	0.3

on the adsorbent's heterogeneous surface. Also, Temkin and D-R isotherm models are not suitable due to their data dispersion and low correlation coefficient. Furthermore, in the Freundlich model, the n value was determined 0.61 for sulfate ion adsorption which indicates that sulfate ion adsorption mechanism through Lotus leaf adsorbent is physical. The R_L values at sulfate ion concentrations between 20 and 120 mg/L were obtained between 0 and 1. The R_L values show that the adsorption process is desirable and reversible.

3. 8. Thermodynamic Study

Thermodynamic parameters include enthalpy changes (ΔH_{ads}), entropy (ΔS_{ads}) and Gibbs free energy (ΔG_{ads}); they have special importance for describing adsorption process and achieving a reaction equilibrium. Whenever there is an adsorption equilibrium constant, then, the thermodynamic functions can be evaluated through equations 7 to 9.[32–33]

$$K = \frac{C_{AS}}{C_A} = \frac{q_e}{C_e} \quad (7)$$

$$\Delta G_{ads} = -RTLnK \quad (8)$$

Also, (ΔH_{ads}) and (ΔS_{ads}) can be calculated through equation 9 from the slope and interface of LnK against 1/T plot.

$$LnK = \frac{\Delta S_{ads}}{R} - \frac{\Delta H_{ads}}{RT} \quad (9)$$

The equilibrium constant is calculated at any temperature using equation 7.

The thermodynamic data graph of sulfate ion adsorption process by activated carbon is shown in Fig. 12. Also, the extracted data from this graph is presented in Table 4. According to the data presented in Table 4, ΔH_{ads}, ΔS_{ads} and ΔG_{ads} values are negative. Therefore, sulfate ion adsorption process by activated carbon is spontaneous. Given being negative, its adsorption percentage decreases with increasing temperature. Considering the enthalpy changes in anion's adsorption on the activated carbon surface, it can be said that the adsorption process is physical; because ΔH < 40 Kj/mol. Since the adsorption process is exothermal, according to le Chatelier principle, it decreases with increasing temperature which is somehow accompanied by irregularities reduction. Moreover, Gibbs free energy for sulfate ions decreased by increasing temperature which indicated that when temperature increases, the amount of spontaneous adsorption process for anion decreases.

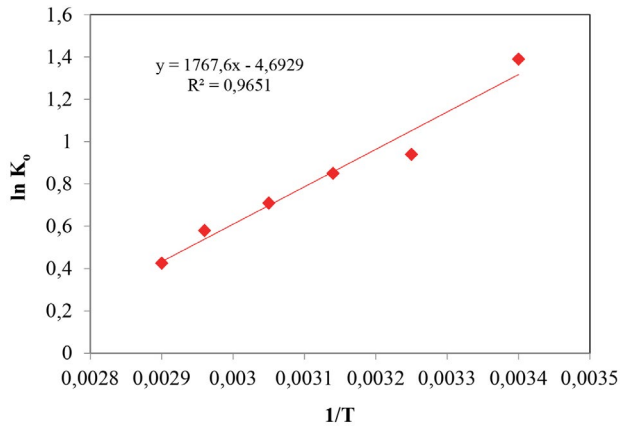

Figure 12. The ln K_o diagram versus 1/T for thermodynamic parameters estimation of sulfate ion adsorption from aqueous solution by activated carbon

3. 9. Kinetic Study of the Adsorption Process

The adsorption kinetic study is highly important because it provides valuable information on the reaction

Table 4. Thermodynamic functions of 100 mg/L SO_4^{2-} ion on the activated carbon surface derived from Lotus leaf (Other terms: m = 0.5 g, pH = 6, Tc = 65min)

T(K)	**K**	**ΔG_{ads} (kJ/mol)**	**ΔH_{ads} (kJ/mol)**	**ΔS_{ads} (kJ/mol)**
298	4.15	−3.44	−15.12	−40.09
308	2.6	−2.4		
318	2.33	−2.31		
328	2.03	−1.94		
338	1.87	−1.63		
348	1.5	−1.16		

pathway and the control mechanism of the adsorption process.[23] In this study, first and second-order pseudo kinetic models were used for kinetic evaluation of sulfate ion on the activated carbon adsorbent. The linear form of the first and second-order kinetic models are presented in terms of equations 10 and 11, respectively:[35–37]

$$\log(q_{e/exp} - q_t) = \log q_{e/cal} - \frac{K_1}{2.303}t \quad (10)$$

$$\frac{t}{q_t} = \frac{1}{K_2 q_{e/cal}^2} + \frac{t}{q_{e/cal}} \quad (11)$$

Here, K_1 pseudo-first-order reaction rate constant, K_2 pseudo-second-order reaction rate constant, $q_{e/cal}$ computational equilibrium adsorption capacity (mg/g), $q_{e/exp}$ empirical equilibrium adsorption capacity (mg/g), q_t adsorption capacity at the time t (mg/g) and t is the time (minute). In order to determine the reaction rate constant of K_1 and $q_{e/cal}$, the $\log(q_{e,exp} - qt)$ graph was drawn based on t and in order to determine the reaction rate constant of K_2 and $q_{e/cal,}$ in the second-order kinetic equation, the t/q_t graph based on t was used.

The kinetic study results are shown in Table 5 and Fig. 13. By comparing the kinetic models' correlation coefficient (R^2), we can say that the kinetics of sulfate ion adsorption on the activated carbon derived from lotus leaves has the most conformity with the second-order pseudo model. Also, the K_1 value in the first-order pseudo model is less than K_2second-order pseudo model. Therefore, sulfate ions adsorption through lotus leaves adsorbent follows the second-order kinetic model.

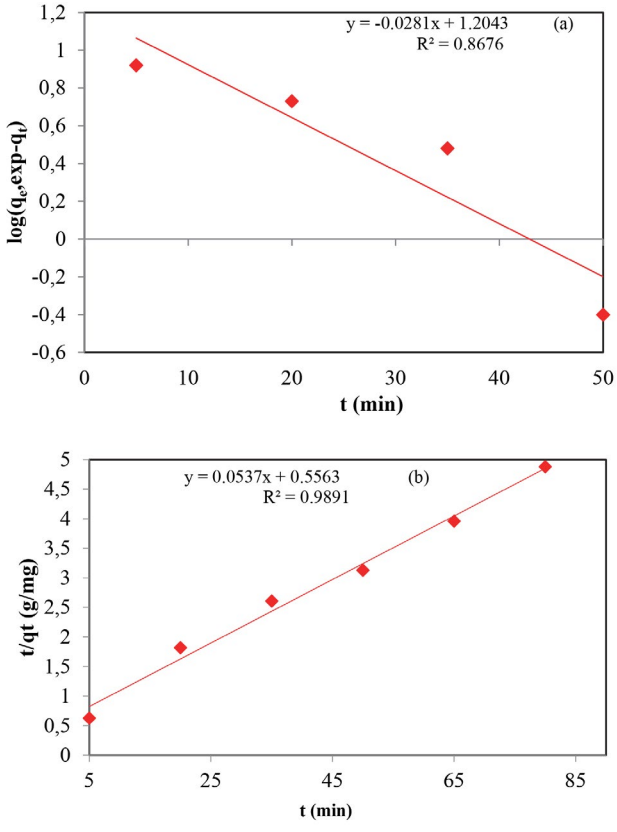

Figure 13. First-order kinetic (a) and second-order kinetic models (b) of SO_4^{2-} ion adsorption on the activated carbon surface derived from Lotus leaf

Table 5. Results of kinetic adsorption models of 100 mg/L SO_4^{2-} ion on the activated carbon surface derived from Lotus leaf (Other terms: T = 328 k, m = 0.5 g, pH = 6, Tc = 65min)

Kinetic models	Parameter	value
Pseudo second-order	$q_{e,cal}$ (mg/g)	16
	K_1 (min^{-1})	0.065
	R^2	0.8676
Pseudo second-order	$q_{e,cal}$ (mg/g)	18.62
	K_2 (g/mg min)	5.2
	R^2	0.9891

4. Conclusion

In this study, sulfate ion adsorption from aqueous solutions through activated carbon adsorbent in the Lotus leaf was studied. Initially, activated carbon adsorbent was prepared and SEM, FTIR, BET, XRD, EDAX analyses were used to determine its surface properties. Then, the effect of various parameters such as pH, temperature, contact time, initial sulfate ion concentration and adsorbent dose on the sulfate ion removal from aqueous solutions through adsorbent was investigated. The results showed that the highest sulfate ion removal efficiency occurs at pH = 6, Tc = 65 min, temperature = 25 °C, initial concentration of 20 mg/L and the adsorbent dose of 5 g/L. After determining the optimum terms, the isotherm, kinetics and thermodynamic behavior of the adsorption process was studied. Langmuir, Freundlich, Temkin and Dubinin-Radushkevich isotherm models were considered to study the adsorption process behavior. The results showed that the Langmuir isotherm model can better describe the equilibrium behavior of the adsorption process due to a higher correlation coefficient. Also, it was determined that sulfate ion adsorption process through lotus leaf adsorbent is physical. During the kinetic models examination, the first and second- order pseudo kinetics models were investigated. The kinetic analysis of the adsorption process was performed using laboratory data at different contact times. The results showed that the second-order pseudo kinetics model has a higher correlation coefficient. The thermodynamic adsorption behavior of sulfate ion through adsorbent was also studied. According to the results, Gibbs free energy for sulfate ions was obtained negative which represents that the adsorption process is possible and spontaneous. Also, the negative amount of enthalpy showed that the adsorption process

was exothermal. Since the adsorption process is exothermal, according to le Chatelier principle, it decreases when temperature raises which is somehow accompanied by a decrease in irregularity. In addition, the amount of entropy was negative showing that the adsorption process is spontaneous.

Conflict of Interests Statement

The authors declare that there is no conflict of interests.

5. References

1. F. Ahmadi, H. Esmaeili. *Desalin. Water Treat.* **2018**, *110*, 154–167. **DOI:**10.5004/dwt.2018.22228
2. R. Mahini, H. Esmaeili, R. Foroutan. *Turk. J. Biochem.* **2018**, *43*, 623–631. **DOI:**10.1515/tjb-2017-0333
3. L. W. H. Pol, P. N. L. Lens, A. J. M. Stams, G. Lettinga. *Biodegradation* **1998**, 9, 213–222. **DOI:**10.1023/A:1008307929134
4. A. Teimouri, H. Esmaeili, R. Foroutan, B. Ramavandi. *Korean J. Chem. Eng.* **2018**, *35*, 479–488. **DOI:**10.1007/s11814-017-0311-y
5. J. Y. park, Y. J. Yoo. *Appl. Microbiol. Biotechnol*. **2009**, *82*, 415–429. **DOI:**10.1007/s00253-008-1799-1
6. H. Demiral, G. Gunduzogla. *Bioresour. Technol.* **2010**, *101*, 1675–1680. **DOI:**10.1016/j.biortech.2009.09.087
7. A. Goshadrou, A. Mohed. *Desalination*. **2010**, *269*, 170–176. **DOI:**10.1016/j.desal.2010.10.058
8. X. Wang, L. Chen, L. Wang, Q. Fan, D. Pan, J. Li, F. Chi, Y. Xie, S. Yu, C. Xiao, F. Luo, J. Wang, X. Wang, C. Chen, W. Wu, W. Shi, S. Wang, X. Wang. *Sci. China Chem*. **2019**, *62*, 933–967. **DOI:**10.1007/s11426-019-9492-4
9. X. Liu, R. Ma, X. Wang, Y. Ma, Y. Yang, L. Zhuang, S. Zhang, R. Jehan, J. Chen, X. Wang. *Environ. Pollut*. **2019**. **DOI:**10.1016/j.envpol.2019.05.050
10. S. M. Mousavi, S. A. Hashemi, A. M. Amani, H. Esmaeili, Y. Ghasemi, A. Babapoor, F. Mojoudi, O. Arjomand. *Phys. Chem. Res*. **2018**, *6*, 759–771.
11. Y. Wu, H. Pang, Y. Liu, X. Wang, S. Yu, D. Fu, J. Chen, X. Wang. *Environ. pollution*. **2019**, *246*, 608–620. **DOI:**10.1016/j.envpol.2018.12.076
12. Q. Huang, S. Song, Z. Chen, B. Hu, J. Chen, X. Wang. *Biochar*. **2019**, *1*, 45–73. **DOI:**10.1007/s42773-019-00006-5
13. M. J. Akhtar, S. Ullah, I. Ahmad, A. Rauf, S. M. Nadeem, M. Y. Khan, S. Hussain, L. Bulgariu. *Chemosphere.* **2018**, *190*, 234–242. **DOI:**10.1016/j.chemosphere.2017.09.136
14. G. Nacu, D. Bulgariu, M. Cristina Popescu, M. Harja, D. Toader Juravle, L. Bulgariu. *Desalin. Water Treat*. **2016**, *57*, 21904–21915. **DOI:**10.1080/19443994.2015.1128366
15. V. K. Gupta, I. Ali. *J. Colloid Interface Sci*. **2004**, *271*, 321–331. **DOI:**10.1016/j.jcis.2003.11.007
16. Z. Khademi, B. Ramavandi, M. T. Ghaneian. *J. Environ. Chem. Eng*. **2015**, *3*, 2057–2067. **DOI:**10.1016/j.jece.2015.07.012
17. S. M. Mousavi, S. A. Hashemi, H. Esmaeili, A. M. Amani, F. Mojoudi. *Acta Chim. Slov.* **2018**, *65*, 750–756. **DOI:**10.17344/acsi.2018.4536
18. L. A. Rodrigues, M. L. C. P. da Silva, M. O. Alvarez-Mendes, Ad. R. Coutinho, G. P. Thim. *Chem. Eng. J*. **2011**, *174*, 49–57. **DOI:**10.1016/j.cej.2011.08.027
19. K. K. Singh, R. Rastogi, S. H. Hasan. *J. Colloid Interface Sci.* **2005**, *290*, 61–68. **DOI:**10.1016/j.jcis.2005.04.011
20. S. H. Min, J. S. Han, E. W. Shin, J. K. Park. *Water Res*. **2004**, *38*, 1289–1296. **DOI:**10.1016/j.watres.2003.11.016
21. M. Martınez, N. Miralles, S. Hidalgo, N. Fiol, I. Villaescusa, J. Poch. *J. Hazard. Mater*. **2006**, *133*, 203–211. **DOI:**10.1016/j.jhazmat.2005.10.030
22. V. K. Gupta, C. K. Jain, I. Ali, M. Sharma, V. K. Saini. *Water Res*. **2003**, *37*, 4038–4047. **DOI:**10.1016/S0043-1354(03)00292-6
23. J. Anwar, U. Shafique, M. Salman, A. Dar, S. Anwar. *Bioresour. Technol*. **2010**, *101*, 1752–1762. **DOI:**10.1016/j.biortech.2009.10.021
24. E. I. El-Shafey. *J. Hazard. Mater*. **2007**, *147*, 546–556 **DOI:**10.1016/j.jhazmat.2007.01.051
25. A. O. Zer, C. Pirinc. *J. Hazard. Mater.* **2006**, *137*, 849–858 **DOI:**10.1016/j.jhazmat.2006.03.009
26. R. A. K. Rao, M. A. Khan, F. Rehman. *Chem. Eng. J.* **2010**, *156*, 106–113. **DOI:**10.1016/j.cej.2009.10.005
27. M. Harja, G. Buema, L. Bulgariu, D. Bulgariu, D. M. Sutiman, G. Ciobanu. *Korean J. Chem. Eng*. **2015**, *32*, 1804–1811. **DOI:**10.1007/s11814-015-0016-z
28. M. Shams, I. Nabipour, S. Dobaradaran, B. Ramavandi, M. Qasemi, M. Afsharnia. *Fresen. Environ. Bull*. **2013**, *22*, 723–727.
29. S. Tamjidi, H. Esmaeili, *Chem. Eng. Technol*. **2019**, *42*, 607–616. **DOI:**10.1002/ceat.201800488
30. L. S. Panchakarla, A. Govindaraj, C. N. R. Rao. *Inorg. Chim. Acta*. **2010**, *363*, 4163–4174. **DOI:**10.1016/j.ica.2010.07.057
31. V. J. Larson, H. H. Schierup. *J. Environ. Qual*. **1981**, *10*, 188–193. **DOI:**10.2134/jeq1981.00472425001000020013x
32. I. Volf, N. G. Rakoto, L. Bulgariu. *Sep. Sci. Technol*. **2015**, *50*, 1577–1586. **DOI:**10.1080/01496395.2014.978018
33. D. Bulgariu, L. Bulgariu. *Bioresour. Technol.* **2012**, *103*, 489–493. **DOI:**10.1016/j.biortech.2011.10.016
34. H. Esmaeili, R. Foroutan. *J. Dispers. Sci. Technol.* **2018**. **DOI:**10.1080/01932691.2018.1489828
35. L. Bulgariu, D. Bulgariu, M. Macoveanu. *Sep. Sci. Technol.* **2011**, *46*, 1023–1033. **DOI:**10.1080/01496395.2010.536192
36. R. Foroutan, H. Esmaeili, S. M. D. Rishehri, F. Sadeghzadeh, S. R. Mirahmadi, M. Kosarifard, B. Ramavandi. *Data Brief*. **2017**, *12*, 485–492. **DOI:**10.1016/j.dib.2017.04.031
37. G. Nacu, L. N. Nemes, L. Bulgariu. *Rev. Roum. Chim*. **2017**, *62*, 439–447.

Povzetek

V članku so preučevali potencial aktivnega oglja pridobljenega iz listov lotusa *Ziziphus spina-christi* za odstranjevanje sulfatnih ionov iz vodnih raztopin. S tem namenom so preučili vpliv različnih parametrov kot so pH vrednost, kontaktni čas, temperatura, koncentracija adsorbenta in začetna koncentracija sulfatnih ionov. Rezultati so pokazali, da je bila največja adsorpcijska učinkovitost (84.5 %) dosežena pri pH vrednosti 6, koncentraciji adsorbenta 5 g/L, koncentraciji sulfatnih ionov 20 ppm, *času 65 min in temperaturi* 45 °C. Študija adsorpcijskega ravnotežja je pokazala, da lahko proces opišemo z Langmuirjevo adsorpcijsko izotermo z maksimalno kapaciteto vezave 9.3 mg/g. Termodinamska študija je pokazala, da je proces adsorpcije na površino aktivnega oglja spontan in eksotermen, kinetiko adsorpcije pa lahko opišemo z modelom psevdo-drugega reda.